

‘Algorithmic cooling’ in a momentum state quantum computer

Tim Freegarde*

Dipartimento di Fisica, Università di Trento, 38050 Povo (TN), Italy

Danny Segal

Quantum Optics and Laser Science, Imperial College, London SW7 2BZ, U.K.

(Dated: December 3, 2018)

We describe a quantum computer based upon the coherent manipulation of two-level atoms between discrete one-dimensional momentum states. Combinations of short laser pulses with kinetic energy dependent free phase evolution can perform the logical invert, exchange, CNOT and Hadamard operations on any qubits in the binary representation of the momentum state, as well as conditional phase inversion. These allow a binary right-rotation, which halves the momentum distribution in a single coherent process. Fields for the coherent control of atomic momenta may thus be designed as quantum algorithms.

PACS numbers: 03.67.Lx, 32.80.Pj, 33.80.Ps, 39.20.+q

Proposed schemes for quantum computation [1] have tended, quite naturally, to focus on quantum analogues of classical binary computing elements. The nuclear spins of a molecule, or of an ensemble of trapped atoms or ions, thus mimic the bits of a conventional computer. In this article, we address a less obvious system, in which information is represented by the momentum of a single atom or molecule, which is manipulated using laser pulses in a one-dimensional geometry that restricts each species to a ladder of equally spaced momentum states. Although any one laser pulse can change the species momentum, through photon absorption and stimulated emission, by only a single photon impulse, we find that sequences of pulses, interspersed with periods of momentum-dependent phase evolution, allow a full suite of quantum computational operations on the qubits comprising the binary representation of the momentum state.

The size of the momentum state quantum computer grows in proportion to the number of quantum states included, where conventional candidates instead scale with the number of qubits representing those states. The number of laser pulses needed to perform each logical operation increases similarly and, although the overall duration proves to be less drastically affected, momentum state systems therefore hold limited promise for real computing. Nonetheless, the scheme outlined here is based upon simple and readily-available elements, albeit in complex combinations, and could thus complement NMR systems [2, 3] as a testbed for experimental studies.

It is, however, in the design of complex fields for coherent control that we foresee the greatest potential, for if momentum-changing operations can form the basis of a quantum computer then the pulse sequences for optical manipulation may be optimized as quantum computational algorithms. In this respect, the momentum state quantum computer is an enthusiastic development of schemes for interferometric cooling [4] and the coherent amplification of laser cooling [5].

Our scheme is based upon the motion in one dimension (henceforth taken to be vertical) of a sample of two-level atoms, such as an atomic beam interacting with transversely propagating laser beams, as shown in Fig. 1. We shall refer to four coherent operations:

$W_+(\alpha, \phi)$	a short upward laser pulse
$W_-(\alpha, \phi)$	a short downward laser pulse
$F(\omega t)$	free evolution (electronic energy)
$G(t/\tau)$	free evolution (kinetic energy),

where $\tau = 2m/(\hbar k^2)$. Here, the short (and therefore spectrally broad) laser pulses couple the upper and lower atomic levels, between which population is transferred through Rabi cycling for the duration of the pulse. Conventionally, we describe the overall effect of the pulse through the phase 2α of the Rabi cycle incurred, the population being inverted when $2\alpha = \pi$ (the so-called ‘ π pulse’), and restored when $2\alpha = 2\pi$. Other fractions of a π pulse will convert an initially pure state into a superposition. The phases ϕ are determined by the relative optical phases of the laser pulses. The free evolution operations $F(\omega t)$ and $G(t/\tau)$ correspond simply to the components of the time-dependent wavefunction phase $\exp(-iEt/\hbar)$ that correspond to the electronic energy and vertical momentum component respectively. Weitz and Hänsch [4] have shown how the electronic and kinetic energy contributions to the free phase evolution may be separated by appropriate insertion of pairs of π -pulses that invert the atomic population, as we discuss later.

In this one-dimensional geometry, the atom is constrained to a ladder of momentum states that are spaced at intervals of the photon momentum $\hbar k = \hbar\omega/c$ (ω being the frequency of the resonant transition) and alternate between the ground and excited electronic levels g and e . We label these states according to their momentum components, in units of the photon impulse $\hbar k$. We initially assume, for our analysis of the momentum state quantum computer, that these momenta take integer values, but this assumption will be relaxed when we later

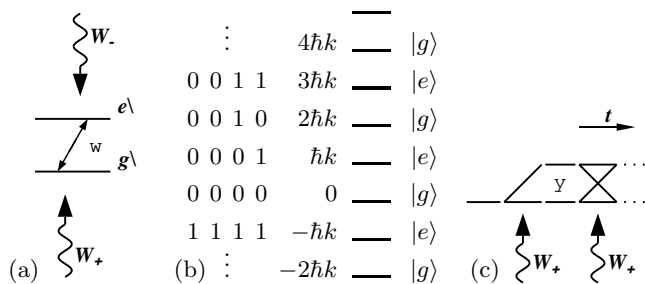


FIG. 1: (a) Fractional π pulses tuned to the two-level atom couple adjacent momentum states, which (b) we label in units of $\hbar k$. This number, in binary representation, gives the qubits of the momentum state quantum computer. (c) Two $\pi/2$ pulses may act as the beamsplitters of an atomic interferometer; the relative phase between the two paths determines whether the pulses add or subtract, and hence whether or not the electronic state is inverted.

consider the consequences for atomic manipulation.

We now convert our representation of the ladder of states to binary, using the notation $Q_n \dots Q_2 Q_1 Q_0$, with the least significant bit on the right. This is the crucial step in our analysis; yet, apart from the correspondence of Q_0 to the electronic state of the atom, binary representation seems at first rather unpromising, for computational notation usually helps only when the bits themselves can be manipulated. While the momentum-changing laser pulses here move population by at most one state at a time, however, appropriate combinations prove to offer exactly such bit-wise manipulation.

The key, as in the interferometric cooling scheme of Ref. [4], is the dependence of the phase of free evolution upon the momentum. For two levels $p + \Delta p/2$ and $p - \Delta p/2$ (in units of $\hbar k$) and electronic energy difference $E_{21} = \hbar\omega$, the relative phase ψ evolves according to

$$\begin{aligned} \psi &= \frac{E_{21}t}{\hbar} + \frac{(\hbar k)^2 t}{2m\hbar} \left[\left(p + \frac{\Delta p}{2} \right)^2 - \left(p - \frac{\Delta p}{2} \right)^2 \right] \\ &= \omega t + \frac{\hbar k^2 t}{m} p \Delta p. \end{aligned} \quad (1)$$

Any pair of momentum states thus incur a relative phase that evolves according to their average momentum p . Cancellation of the electronic contribution to the phase, by inserting π pulse pairs so that the states spend equal times in the ground and excited levels [4], merely changes the average Δp and hence the rate at which this proceeds.

We illustrate the capacity for bit-wise manipulation with the example of a three qubit right rotation,

$$\{Q_2, Q_1, Q_0\} \rightarrow \{Q_0, Q_2, Q_1\}.$$

In our largely diagrammatic description, which has its origins in Fig. 1(c), pulses or complete pulse sequences coupling adjacent levels are indicated by \otimes when they produce a superposition (e.g., a $\pi/2$ pulse), \times when they

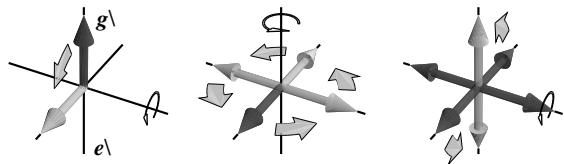


FIG. 2: Bloch-vector representation of the first stage (Eq. (2)) of the right-rotation. The first pulse rotates the four ground states into the horizontal plane; free evolution distributes these around the vertical axis according to their momenta; the second pulse then returns two to pure states, leaving the others in mixed states. Aside from phase corrections, the full right-rotation operation takes $18 \pi/2$ pulses and 26π pulses.

cause inversion (the π pulse) and \otimes when $2\alpha = 0, 2\pi$ and so on. For periods of free evolution, we simply indicate the relative phases introduced between coupled states.

First consider a pair of upward-travelling $\pi/2$ pulses, separated by a period of free evolution that introduces between coupled states a relative phase adjusted to give in each case an integer power of $\exp(-i\pi/2)$. This forms a simple interferometer which, depending upon the original state momentum, can invert population, return it to its original state, or leave initially pure states coupled (see Fig. 1(c)). The sequence repeats every $8\hbar k$.

$$\begin{array}{c} 7 \text{ --- } |e\rangle \\ 6 \text{ --- } |g\rangle \\ 5 \text{ --- } |e\rangle \\ 4 \text{ --- } |g\rangle \\ 3 \text{ --- } |e\rangle \\ 2 \text{ --- } |g\rangle \\ 1 \text{ --- } |e\rangle \\ 0 \text{ --- } |g\rangle \end{array} \left\{ \begin{array}{ccc} \otimes & 2\pi & \otimes \\ \otimes & \frac{3\pi}{2} & \otimes \\ \otimes & \pi & \otimes \\ \otimes & \frac{\pi}{2} & \otimes \end{array} \right\} \equiv \begin{array}{c} \times \\ \otimes \\ \text{---} \\ \text{---} \\ \otimes \end{array} \quad (2)$$

This and subsequent operations may be visualized, as in Fig. 2, as rotations of Bloch vectors representing the coupled states - a picture also suitable for NMR computers [6, 7]. Pure states are vertically up ($|g\rangle$) or down ($|e\rangle$), and are coupled by rotation about a horizontal axis, whose direction depends upon the optical phase. Free evolution corresponds to rotation about the vertical axis.

Two such sequences may now be combined with a further momentum-dependent phase between them to form a second interferometer for the states left in superpositions. The ladder of phases is offset either via the $F(\omega t)$ operation (such as a period of uncompensated free evolution that is dominated by the ‘electronic’ phase), or by appropriate phasing of the subsequent laser pulses. The

result is a conditional state exchange:

$$\begin{array}{c}
 7 \text{ --- } |e\rangle \\
 6 \text{ --- } |g\rangle \\
 5 \text{ --- } |e\rangle \\
 4 \text{ --- } |g\rangle \\
 3 \text{ --- } |e\rangle \\
 2 \text{ --- } |g\rangle \\
 1 \text{ --- } |e\rangle \\
 0 \text{ --- } |g\rangle
 \end{array}
 \left\{ \begin{array}{ccc}
 \times & \frac{5\pi}{2} & \times \\
 \otimes & 2\pi & \otimes \\
 \text{---} & \frac{3\pi}{2} & \text{---} \\
 \otimes & \pi & \otimes
 \end{array} \right\} \equiv \begin{array}{c}
 \text{---} \\
 \text{---} \\
 \times \\
 \text{---} \\
 \text{---} \\
 \text{---} \\
 \text{---} \\
 \text{---}
 \end{array} \quad (3)$$

Precisely which pair of adjacent states is exchanged by this operation depends upon the directions and relative phases of the $\pi/2$ pulses. As the penultimate step, we construct the two-qubit exchange operation EX(2,1):

$$\begin{array}{c}
 7 \text{ --- } |e\rangle \\
 6 \text{ --- } |g\rangle \\
 5 \text{ --- } |e\rangle \\
 4 \text{ --- } |g\rangle \\
 3 \text{ --- } |e\rangle \\
 2 \text{ --- } |g\rangle \\
 1 \text{ --- } |e\rangle \\
 0 \text{ --- } |g\rangle
 \end{array}
 \left\{ \begin{array}{ccc}
 \text{---} & \text{---} & \text{---} \\
 \text{---} & \text{---} & \text{---} \\
 \text{---} & \times & \text{---} \\
 \times & \text{---} & \times \\
 \text{---} & \times & \text{---} \\
 \text{---} & \text{---} & \text{---} \\
 \text{---} & \text{---} & \text{---} \\
 \text{---} & \text{---} & \text{---}
 \end{array} \right\} \equiv \begin{array}{c}
 \text{---} \\
 \text{---} \\
 \times \\
 \times \\
 \times \\
 \text{---} \\
 \text{---} \\
 \text{---}
 \end{array} \quad (4)$$

The right-rotation RR3 is completed by combining this sequence with the much simpler exchange EX(1,0) of qubits Q_1 and Q_0 . This is given in Table I together with a range of other operations on the first three qubits from which, in conjunction with the one-bit operations $W_+(\alpha, \phi)$ and $F(\omega t)$, a complete set may be formed [8].

When only the ground electronic level is occupied ($Q_0 = 0$), the right-rotation is indistinguishable from a divide-by-two operation (e.g., $100(=4) \rightarrow 010(=2)$) and provides a cooling mechanism. As shown in Fig. 3, the four ground states are coherently mapped onto the four lowest momentum states, two of which subsequently undergo spontaneous emission, leaving only states 0, 2 and 4 populated. The coherent process, which pumps heat from kinetic to electronic energy, may then be repeated, further narrowing the momentum distribution.

At this point, we relax our earlier assumption of integer-valued momentum states, and find that the effect, whilst imperfect for non-integer momenta, nonetheless remains. The results of our simulations for the effect of this sequence on an initially flat distribution across fractional momentum states are shown in Fig. 4.

For our simulations, we have used matrix representations of the pulse and evolution operations. Although the matrices are in principle infinite, all non-zero terms cluster around the leading diagonal and any element $m_{i,j}$ differs from the diagonally displaced term $m_{i+2n,j+2n}$ only through its momentum dependence, so we may summarize the matrices as 4×4 elements, given below and derived from the equations of Friedberg and Hartmann [9].

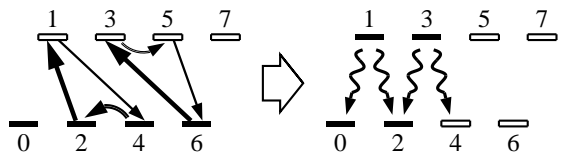


FIG. 3: Cooling via the right-rotation operation, shown here applied to the lowest three qubits. The initial distribution across ground states $\{0, 2, 4, 6\}$ is transferred (bold arrows) to the lowest momentum states $\{0, 1, 2, 3\}$; subsequent spontaneous emission leaves population in states $\{0, 2, 4\}$. The width of the momentum distribution may thus be reduced by a factor of nearly 2 in a single coherent step.

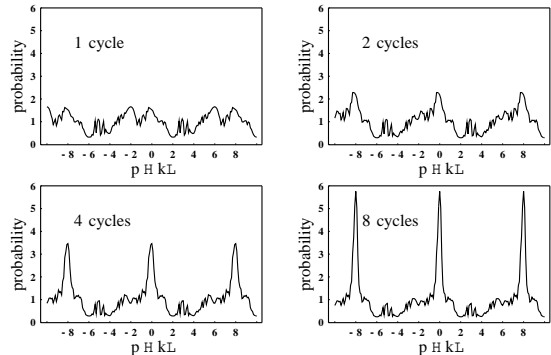


FIG. 4: Simulated evolution of the momentum state distribution, shown after 1, 2, 4 and 8 cycles of the 3-qubit coherent cooling algorithm. Although the process applies perfectly only to atoms with even, integral momenta, significant cooling remains apparent. Spontaneous emission scrambles the exact momenta. After only a few coherent cycles, the distribution has been narrowed to less than a single photon impulse. The initial probability density is unity.

Matrices that we use in practice must merely be expanded to cover the sequence of interactions and the momentum range that we wish to describe. The following matrices act on the states $\{2, 1, 0, -1\}$.

For upward and downward travelling fractional π pulses corresponding to Bloch vector rotation through ‘Rabi angle’ 2α and optical phase ϕ , we have

$$W_+(\alpha, \phi) = \begin{pmatrix} \cos \alpha & 0 & 0 & 0 \\ 0 & \cos \alpha & ie^{i\phi} \sin \alpha & 0 \\ 0 & ie^{-i\phi} \sin \alpha & \cos \alpha & 0 \\ 0 & 0 & 0 & \cos \alpha \end{pmatrix} \quad (5)$$

and

$$W_-(\alpha, \phi) = \begin{pmatrix} \cos \alpha & ie^{-i\phi} \sin \alpha & 0 & 0 \\ ie^{i\phi} \sin \alpha & \cos \alpha & 0 & 0 \\ 0 & 0 & \cos \alpha & ie^{-i\phi} \sin \alpha \\ 0 & 0 & ie^{i\phi} \sin \alpha & \cos \alpha \end{pmatrix}. \quad (6)$$

The matrices for free evolution according to the electronic

and kinetic energies are respectively

$$F(\omega t) = \begin{pmatrix} 1 & 0 & 0 & 0 \\ 0 & e^{-i\omega t} & 0 & 0 \\ 0 & 0 & 1 & 0 \\ 0 & 0 & 0 & e^{-i\omega t} \end{pmatrix} \quad (7)$$

and

$$G\left(\frac{t}{\tau}\right) = \begin{pmatrix} e^{-i(p_0+2)^2 t/\tau} & 0 & 0 & 0 \\ 0 & e^{-i(p_0+1)^2 t/\tau} & 0 & 0 \\ 0 & 0 & e^{-ip_0^2 t/\tau} & 0 \\ 0 & 0 & 0 & e^{-i(p_0-1)^2 t/\tau} \end{pmatrix} \quad (8)$$

where $\tau = 2m/(\hbar k^2)$. Weitz and Hänsch's sequence for interferometric cooling thus becomes

$$W_+\left(\frac{\pi}{4}\right) \cdot G\left(\frac{2T-T'}{\tau}\right) \cdot F(\omega(2T-T')) \cdot W_-\left(\frac{\pi}{2}\right) \cdot G\left(\frac{2T}{\tau}\right) \cdot F(2\omega T) \cdot W_-\left(\frac{\pi}{2}\right) \cdot G\left(\frac{T'}{\tau}\right) \cdot F(\omega T') \cdot W_+\left(\frac{\pi}{4}\right)$$

No attempt has yet been made to optimize the sequences given here: the phase corrections often serve only to demonstrate the exact equivalence to a quantum computer, and reductions in the complexity, duration or momentum sensitivity of each operation should be possible. Nor have we examined superpositions involving more than two states [10] or interactions at more than one wavelength [11]. Instead of the fractional Rabi coupling of electronic transitions assumed for simplicity, our scheme could be more robustly implemented using Raman transitions [12] for adiabatic passage [13, 14] between Zeeman or hyperfine levels, possible even with modulated c.w. lasers [15]. The scheme, which we think of as a form of 'algorithmic cooling' [16] in its broadest sense, could in principle be extended to three dimensions. Owing to the non-resonant nature of the pulsed interactions, it would also be suitable for molecules, for which

the large impulse per coherent cycle would be a particular advantage.

* Electronic address: tim.freegarde@physics.org

- [1] D. Deutsch, Proc. Royal Soc. London A **400**, 97 (1985).
- [2] I. L. Chuang, N. Gershenfeld, and M. Kubinec, Phys. Rev. Lett. **80**(15), 3408 (1998).
- [3] J. A. Jones, M. Mosca, and R. H. Hansen, Nature **393**(6683), 344 (1998).
- [4] M. Weitz and T. W. Hänsch, Europhys. Lett. **49**(3), 302 (2000).
- [5] T. Freegarde and D. Segal, in preparation (2002).
- [6] N. A. Gershenfeld and I. L. Chuang, Science **275**, 350 (1997).
- [7] J. A. Jones, R. H. Hansen, and M. Mosca, J. Magnetic Resonance **135**, 353 (1998).
- [8] A. Barenco, C. H. Bennett, R. Cleve, D. P. DiVincenzo, N. Margolus, P. Shor, T. Sleator, J. A. Smolin, and H. Weinfurter, Phys. Rev. A **52**(5), 3457 (1995).
- [9] R. Friedberg and S. R. Hartmann, Phys. Rev. A **48**(2), 1446 (1993).
- [10] H. Hinderthür, F. Ruschewitz, H.-J. Lohe, S. Lechte, K. Sengstock, and W. Ertmer, Phys. Rev. A **59**(3), 2216 (1999).
- [11] J. Söding, R. Grimm, Y. B. Ovchinnikov, P. Bouyer, and C. Salomon, Phys. Rev. Lett. **78**(8), 1420 (1997).
- [12] D. S. Weiss, B. C. Young, and S. Chu, Phys. Rev. Lett. **70**(18), 2706 (1993).
- [13] M. Weitz, B. C. Young, and S. Chu, Phys. Rev. Lett. **73**(19), 2563 (1994).
- [14] P. D. Featonby, G. S. Summy, C. L. Webb, R. M. Godun, M. K. Oberthaler, A. C. Wilson, C. J. Foot, and K. Burnett, Phys. Rev. Lett. **81**(3), 495 (1998).
- [15] M. Cashen, O. Rivoire, L. Yatsenko, and H. Metcalf, J. Opt. B **4**, 75 (2002).
- [16] P. O. Boykin, T. Mor, V. Roychowdhury, F. Vatan, and R. Vrijen, Proc. Nat. Acad. Sci. **99**(6), 3388 (2002).

TABLE I: Basic operations of the momentum state quantum computer. No attempt has been made to optimize the pulse sequences, which run from right to left, and some uncorrected phases remain in the operations marked with an asterisk. For the operation G , p_0 is taken to be zero (mod 8).

level	name	description	sequence
basic	$G(t/\tau)$		$W_-(\pi, 0) \cdot FG(t/4\tau) \cdot W_-(\pi, 0) \cdot FG(t/4\tau) \cdot$ $W_+(\pi, 0) \cdot FG(t/4\tau) \cdot W_+(\pi, 0) \cdot FG(t/4\tau)$
1 qubit	NOT(0)	$Q_0 \rightarrow \overline{Q_0}$	$F(\frac{\pi}{2}) \cdot W_+(\frac{\pi}{2}, 0) \cdot F(\frac{\pi}{2})$
	CP1(0)	if state=0, invert phase	$F(\pi) \cdot W_+(\pi, 0)$
	HAD(0)	Walsh-Hadamard on Q_0	$W_+(\frac{\pi}{4}, \frac{\pi}{2}) \cdot F(\pi) \cdot W_+(\pi, 0)$
2 qubit	EX(1,0)	$\{Q_1, Q_0\} \rightarrow \{Q_0, Q_1\}$	$F(\frac{\pi}{2}) \cdot W_-(\frac{\pi}{4}, \pi) \cdot G(\frac{\pi}{4}) \cdot W_-(\frac{\pi}{4}, \frac{\pi}{4}) \cdot F(\frac{5\pi}{4})$
	CNOT(1,0)	$\{Q_1, Q_0\} \rightarrow \{Q_1, Q_1 \oplus Q_0\}$	$F(\frac{\pi}{2}) \cdot W_+(\frac{\pi}{4}, \pi) \cdot G(\frac{\pi}{4}) \cdot W_+(\frac{\pi}{4}, \frac{\pi}{4}) \cdot F(\frac{5\pi}{4})$
	$\overline{\text{CNOT}}$ (1,0)	$\{Q_1, Q_0\} \rightarrow \{Q_1, \overline{Q_1 \oplus Q_0}\}$	$W_+(\pi, 0) \cdot F(\frac{3\pi}{2}) \cdot W_+(\frac{\pi}{4}, 0) \cdot G(\frac{\pi}{4}) \cdot W_+(\frac{\pi}{4}, \frac{\pi}{4}) \cdot F(\frac{5\pi}{4})$
	CP2(0)	if state=0, invert phase	$F(\frac{3\pi}{4}) \cdot G(\frac{\pi}{4}) \cdot W_+(\pi, 0)$
	HAD(1,0)	Walsh-Hadamard on Q_1, Q_0	EX(1,0) · HAD(0) · EX(1,0) · HAD(0)
3 qubit	SW3(2,3)*	swap states 2, 3	$W_+(\frac{\pi}{4}, 0) \cdot G(\frac{\pi}{8}) \cdot W_+(\frac{\pi}{4}, \frac{9\pi}{8}) \cdot F(\frac{5\pi}{4}) \cdot G(\frac{\pi}{8}) \cdot$ $W_+(\frac{\pi}{4}, 0) \cdot G(\frac{\pi}{8}) \cdot W_+(\frac{\pi}{4}, \frac{9\pi}{8}) \cdot F(\frac{13\pi}{8}) \cdot G(\frac{\pi}{4})$
	SW3(3,4)*	swap states 3, 4	$F(\pi) \cdot W_-(\frac{\pi}{4}, 0) \cdot G(\frac{\pi}{8}) \cdot W_-(\frac{\pi}{4}, \frac{5\pi}{8}) \cdot F(\frac{5\pi}{4}) \cdot G(\frac{\pi}{8}) \cdot$ $W_-(\frac{\pi}{4}, 0) \cdot G(\frac{\pi}{8}) \cdot W_-(\frac{\pi}{4}, \frac{5\pi}{8}) \cdot F(\frac{13\pi}{8}) \cdot G(\frac{\pi}{4})$
	SW3(4,5)*	swap states 4, 5	$W_+(\frac{\pi}{4}, 0) \cdot G(\frac{\pi}{8}) \cdot W_+(\frac{\pi}{4}, \frac{5\pi}{8}) \cdot F(\frac{5\pi}{4}) \cdot G(\frac{\pi}{8}) \cdot$ $W_+(\frac{\pi}{4}, 0) \cdot G(\frac{\pi}{8}) \cdot W_+(\frac{\pi}{4}, \frac{5\pi}{8}) \cdot F(\frac{\pi}{8}) \cdot G(\frac{\pi}{4})$
	EX(2,1)	$\{Q_2, Q_1\} \rightarrow \{Q_1, Q_2\}$	$W_+(\pi, 0) \cdot \overline{\text{CNOT}}$ (1,0) · EX(1,0) · $G(\frac{3\pi}{8}) \cdot F(\frac{13\pi}{8}) \cdot$ EX(1,0) · $\overline{\text{CNOT}}$ (1,0) · SW3(3,4) · NOT(0) · $F(\pi)$ · NOT(0) · SW3(4,5) · NOT(0) · $F(\pi)$ · NOT(0) · SW3(2,3) · SW3(3,4) · $G(\frac{3\pi}{8}) \cdot F(\frac{5\pi}{8})$
	RR3	$\{Q_2, Q_1, Q_0\} \rightarrow \{Q_0, Q_2, Q_1\}$	EX(2,1) · EX(1,0)
	RL3	$\{Q_2, Q_1, Q_0\} \rightarrow \{Q_1, Q_0, Q_2\}$	RR3 · RR3
	CP3(0)	if state=0, invert phase	NOT(0) · RL3 · NOT(0) · RL3 · $F(\frac{5\pi}{8}) \cdot G(\frac{3\pi}{8}) \cdot$ RR3 · SW3(4,5) · $F(\frac{3\pi}{2}) \cdot$ SW3(4,5) · $F(\frac{\pi}{2}) \cdot$ NOT(0) · RR3 · NOT(0) · $W_+(\pi, 0)$